

Modelling and Simulation of A Direct Ethanol Fuel Cell: Electrochemical Reactions and Mass Transport Consideration

Christopher Janting Liew Chalu*

Petrochemical Engineering Department, Polytechnic of Kuching Sarawak, Kuching, Malaysia

Abstract

Mathematical modelling was developed for direct ethanol fuel cell (DEFC) by considering electrochemical reactions and mass transport. The model was validated against experimental data from previous research and showed good agreement with the data. The developed mathematical modelling for this research was based on the Butler-Volmer equation, Tafel equation and Fick's law. The model was used to investigate parameters such as ethanol concentration and cell operating temperature. The developed mathematical model simulated the data from previous research. Ethanol concentration played a vital role to achieve high-performance DEFC. The higher the ethanol concentration, the higher current could be generated in DEFC. Nonetheless, the higher the usage of the ethanol concentration, the higher the ethanol crossover might occur. The highest current density produced from the fuel cell was at 21.48 mA cm⁻², for 2M of ethanol concentration. Operating temperature also affected cell performance. The higher the operating temperature, the higher power density could be generated—the peak power density of 5.7 mWcm⁻² at 75 °C with 2M of ethanol. As for ethanol crossover, the highest ethanol crossover was at 12.4 mol m⁻³ for 3M concentration of ethanol. It proved that higher ethanol concentration led to higher ethanol crossover.

Keywords: *Direct ethanol fuel cell, Ethanol crossover, Mass resistance, Mathematical modelling*

1. Introduction

Energy is a vital source to achieve social, economic, environmental and human development. The world depends on coal, petroleum and natural gas to produce energy [1]. However, an energy such as fossil fuel may negatively impact the environment, such as global warming and acidic rain [2]. So, research on renewable energies has been intensified ever since then. Renewable energy such as fuel cell technology produces electrical energy from high-efficiency chemical energy. A direct ethanol fuel cell (DEFC) is one of the fuel cells that produce sustainable energy. Ethanol contains a high density of energy compared to methanol - which is commonly used, and methanol is toxic to humans [3-4]. However, DEFC faces some challenges, such as ethanol crossover [5]. Ethanol crossover is a movement of ethanol from anode to cathode through an electrolyte membrane. Ethanol crossover is wasting fuel throughout the operation. In order to solve ethanol crossover, factor like ethanol mass transfer has to be taken into account.

This research aims to develop a mathematical model for DEFC based on electrochemical reaction and mass transport and simulate and analyse the effect of operating conditions on DEFC

* Corresponding author. Tel.: +082-845596
E-mail address: chrisleu158@gmail.com

Manuscript History:

Received 3 December, 2021, Revised 6 April, 2022, Accepted 21 April, 2022, Published 30 April, 2022

Copyright © 2021 UNIMAS Publisher. This is an open access article under the CC BY-NC-SA 4.0 license.

<https://doi.org/10.33736/jaspe.4592.2022>

performance. Ethanol crossover is a prevalent problem in DEFC. Generally, the rate of ethanol crossover increases with temperature, current density and ethanol concentration at the feed [6]. The higher the ethanol concentration, the higher the ethanol crossover is. A study has shown that ethanol crossover the Nafion membrane at 75 °C at a flow rate of 1.0 mL/min, at ethanol concentration of 1.0M, ethanol crossover rate was at 5×10^{-8} mol/cm².s. While at 2.0M and 4.0M, the rate were at 13×10^{-8} mol/cm².s and 38×10^{-8} mol/cm².s, respectively [7]. The performance of the fuel cell increases when the operating temperature gets higher as ethanol conversion increases with cell current and operating temperature. A study showed that 1M of ethanol concentration, with temperatures of 60 °C, 70 °C, 80 °C and 90 °C, the current density generated was 30 mA cm⁻², 43 mA cm⁻², 57 mA cm⁻² and 82 mA cm⁻², respectively [8]. There are many experimental types of research done for ethanol crossover. Experimental research can be costly. The other alternative for this research is developing mathematical modelling based on the Butler-Volmer equation, Tafel equation and Fick's law. Model simulation can be done with one-dimensional(1D), two-dimensional(2D) and three-dimensional(3D). 1D model is the X-axis through-plane direction, it can be performed by using Microsoft Excel simulation. A study by An et al. [9] that used 1M, 2M and 3M of ethanol concentration increased the current density with ethanol concentration at 2 mA cm⁻², 4.3 mA cm⁻² and 6.5 mA cm⁻², respectively. 2D model is where a code is developed, for example, in Fortran90 software using the finite element method to calculate the flow in different layers of the fuel cell. In a study by De Souza et al. [10], two operating temperatures used were 315K and 363K. The cell voltage increased with increasing temperature at 0.43 V and 0.45 V, respectively. 3D models can predict the flow on all layers of fuel cells and better analyse physical and chemical phenomena inside them. In a study by Gomes & Bortoli [11], at 1M, 2M and 3M of ethanol concentration, the cell voltage increased with ethanol concentration at 0.43 V, 0.45 V and 0.47 V, respectively.

Mathematical modelling is an alternative way to measure and verify the performance of the fuel cell and mass transfer in the fuel cell. The developed mathematical modelling is to study the current density, cell voltage, power density, and molar concentration at each layer of the DEFC. This research was based on a one-dimensional model that studied electrochemical reaction and mass transfer by calculating them using Microsoft Excel. The cell performance could be determined by considering the concentration loss, ohmic loss, and activation loss. A two-dimensional model is more complicated with multiple reaction steps, and a three-dimensional model needs to use software such as computational fluid dynamics methods (CFD). CFD can perform analyses of Reynolds number, which is unnecessary in this research. The parameters used are ethanol concentration and operating temperature.

2. Methods

This study was based on Azam et al. [12] Single-cell DEFC was used in this study, with the membrane electrode assembly (MEA) with 2.5 cm² active area and Nafion membrane 117. First, 0.5 M of ethanol solution was fed to the anode chamber, and the air was flown continuously using a pump at a flow rate of 200mL min⁻¹. Next, different ethanol concentrations (0.5 – 3.0 M) were used at room temperature conditions. Then, the effect of operating temperature was carried out in a humidity chamber, with different operating temperatures (28 °C, 50 °C & 75 °C) used at 2M of ethanol concentration. Ethanol crossover was analysed by using a CO₂ analyser on the cathode side. Ethanol diffused from the anode through the membrane to the cathode side. The crossed over ethanol was oxidised and formed carbon dioxide [13]. The CO₂ was analysed using a CO₂ analyser. DEFC operated for 2 hours in semi-passive mode.

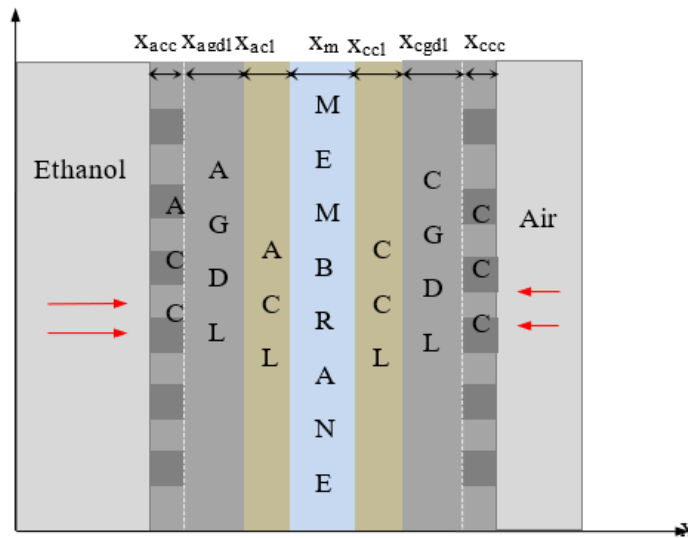


Figure 1. Schematic diagram of DEFC

Figure 1 shows the schematic diagram of DEFC. The change of ethanol concentration at each layer at the anode can be studied through the derived mathematical modelling. The mathematical modelling is derived from the mass balance equation. The equation that relates gas concentration and diffusion coefficient is given by:

$$v \frac{dc}{dx} - D \frac{d^2c}{dx^2} - r = 0 \quad (1)$$

The reaction that occurs is:

$$r = -\frac{zSi(x)}{nFw} \quad (2)$$

Where S is stoichiometry value, $i(x)$ is the current density (Am^{-2}), n is the number of electrons, F is Faraday number, w is the width of the pathway (m), and z is the number of channels. The negative symbol -ve shows a reduction of reaction materials for the reaction.

Butler-Volmer equation is used to derive mathematical modelling for current density generation.

$$i = i_0 \left[\exp\left(\frac{-n\alpha F\eta}{RT}\right) - \exp\left(\frac{n[1-\alpha]F\eta}{RT}\right) \right] \quad (3)$$

Where i_0 is the current density on the surface area per volume of the electrode (Am^{-3}), n number of electrons, a charge transfer coefficient, R gas constant ($\text{kPam}^3\text{kg}^{-1}\text{mol}^{-1}\text{K}^{-1}$), T operating temperature (K), F Faraday constant, dan η cell overpotential (V).

The current density at the anode and cathode of the DEFC is calculated by using the following equation 1 & 2, respectively:

$$i_a = l(ai_{0,a}^{ref} \left[\frac{c_{af}}{c_{af,ref}} \right]^{\frac{1}{2}} \left[\exp\left(\frac{\alpha_a F}{RT} \eta\right) \right]) \quad (4)$$

$$i_c = l(ai_{0,c}^{ref} \left[\frac{C_{O_2}}{C_{O_2,ref}} \right] \left[\exp\left(\frac{\alpha_a F}{RT} \eta\right) \right]) \quad (5)$$

Where $ai_{0,c}^{ref}$ is the reference current density at the surface area per volume of anode electrode (Am^{-3}), $ai_{0,c}^{ref}$ is the reference current density at the surface per volume of cathode electrode (Am^{-3}), and C_{ref} is the reference molar concentration (mol.m^{-3}).

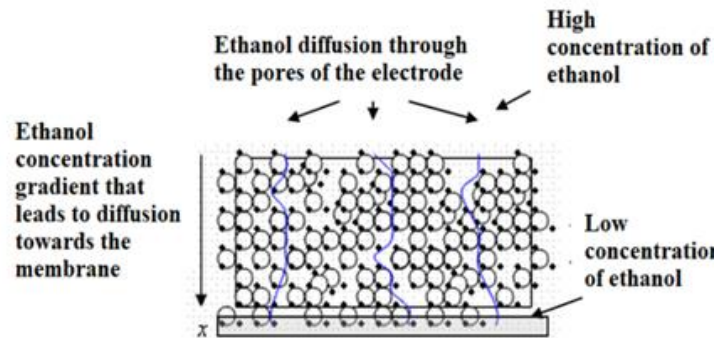


Figure 2. Ethanol crosses the pathway along the MEA

The mass balance equation for molar concentration is derived from:

$$v \frac{dC_e}{dx} = - \frac{zSi_a(x)}{nFw} \quad (6)$$

Figure 2 shows the ethanol crossing the pathway along with the MEA. It is affected by the current density at the specific distance, reaction stoichiometry, number of electrons, rate of reactant reaction and width of the reactant reaction pathway. Equation 6 at the anode is done by combining the derived Butler-Volmer equation for current density and rearranging to relate ethanol concentration change at a certain distance and produce equation 7:

$$\frac{dC_e}{dx} = - \frac{zLai_{0,a}^{ref} \left[\exp\left(\frac{\alpha_a F}{RT} \eta\right) \right] \left[\frac{C_e}{C_{e,ref}} \right]^{0.5}}{nvFw} \quad (7)$$

and also taking into account constant value k_0 :

$$k_0 = \frac{nvFw \left[\exp\left(-\frac{\alpha_a F}{RT} \eta\right) \right]}{zLai_{0,a}^{ref}}$$

Thus, the molar concentration of x-direction of diffusion on the anode and cathode is shown in equations 8 and 9, respectively:

$$C_e = C_{e,0} \left[1 - \frac{0.5}{k_0^*} \left(\frac{x}{L} \right) \right]^2 \quad (8)$$

$$C_{O_2} = C_{O_2,0} \exp \left(-\frac{1}{k_2} \left(\frac{x}{L} \right) \right) \quad (9)$$

Cell potential or cell voltage can be calculated by using the equation 10:

$$E_{cell} = E_{oc} - \eta_{act}^a - \eta_{act}^c - \eta_{ohmic} - \eta_{concentration} \quad (10)$$

$$\eta_{act} = \frac{RT}{2\alpha F} \ln \left(\frac{i}{i_0} \right)$$

$$\eta_{ohmic} = ir$$

$$\eta_{concentration} = -\frac{RT}{2F} \ln \left(1 - \frac{i}{i_l} \right)$$

3. Results and discussion

The data for the mathematical modelling was collected from Azam et al. [12], and the collected data (experimental data) was compared with the one from the simulation model. Model validation based on research data was essential to prove the validity of the derived mathematical model. Validation was done on the operating parameters of the fuel cell - the concentration of the ethanol used and the operating temperature.

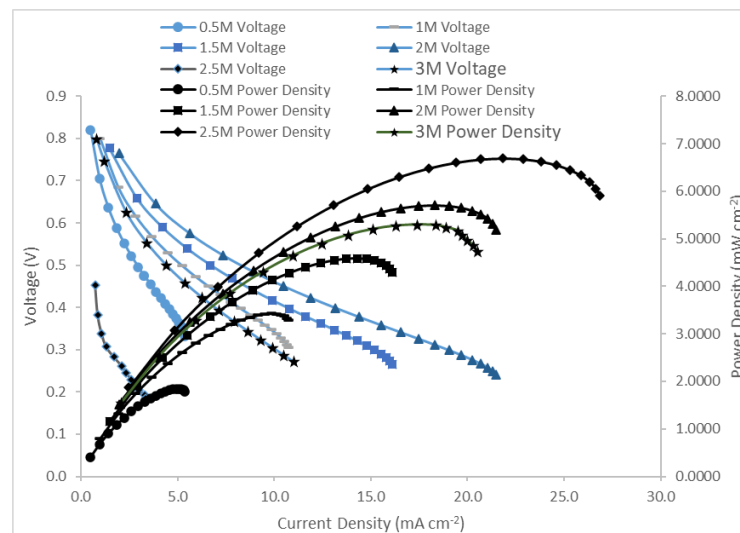


Figure 3. Influence of ethanol concentration on fuel cell performance based on mathematical modelling

The validation of the model simulation was done for the ethanol concentration and operating temperature. Overall, the collected data and values from the model simulation matched and thus

verified the derived mathematical modelling. Figure 3 shows the graph of polarity curves generated from mathematical modelling for 0.5M, 1M, 1.5M, 2M, 2.5M and 3M of ethanol concentration at room temperature. Based on this figure, the performance of the fuel cell increases with ethanol concentration. The cell voltage increased with increasing ethanol concentration and decreased when ethanol concentration reached more than 2M. The increasing cell voltage with the concentration of ethanol was due to an increase in anode reaction rate. Higher ethanol concentration increased the diffusion and concentration of ethanol in the catalyst layer. Hence, the oxidation of ethanol was improved [12].

The reduction of cell voltage with increasing ethanol concentration for more than 2M of ethanol concentration was due to mixed potential resulting from ethanol crossover. Ethanol crossover might cause water transport in the cell as ethanol oxidised to produce water at the cathode side [12]. Ethanol crossover might also reduce the cathode potential and the overall efficiency. It might also poison the catalyst at the cathode and fuel wastage [14].

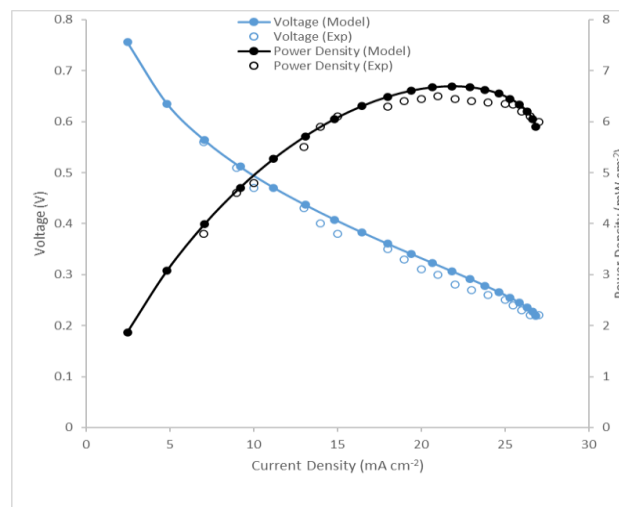


Figure 4. Comparison of experimental and modelling data for 2.5M of ethanol concentration at room temperature

The experimental data were compared with the data generated from mathematical modelling. The data from 2.5M of ethanol concentration were used to compare the cell voltage and power density generated. 2.5M of ethanol concentration was chosen as it produced the highest power density generated among all concentrations used. Polarity curves and power density for comparison between experimental and modelling data at 2.5M of ethanol concentration at room temperature are shown in Figure 4. The voltage and power density values were parallel for experimental and modelling. It showed that mathematical modelling could predict and produce accurate results compared with the experimental data. The error percentage for voltage was 2% and power density at 2.8%, which was low compared to Ismail et al. at 17.5% [15].

The validation of the model simulation was also done for the various operating temperature of the cell. 2M of ethanol concentration was used for the simulation due to the highest cell voltage attained with this concentration, as discussed previously. Figure 5 shows the graph of polarity curves generated from mathematical modelling for 2M of ethanol concentration at 28 °C (room temperature), 50 °C and 75 °C. Based on this figure, the performance of the fuel cell increases with operating temperature. Due to the anode and cathode electrode kinetics, PEM conductivity and mass transfer properties increased with increasing temperature [16]. The temperature increase increased the

hydrogen ions passage through the membrane, which improved the DEFC performance [17]. This modelling showed DEFC giving a peak power density of 5.7 mWcm^{-2} at $75 \text{ }^\circ\text{C}$ with 2M of ethanol concentration.

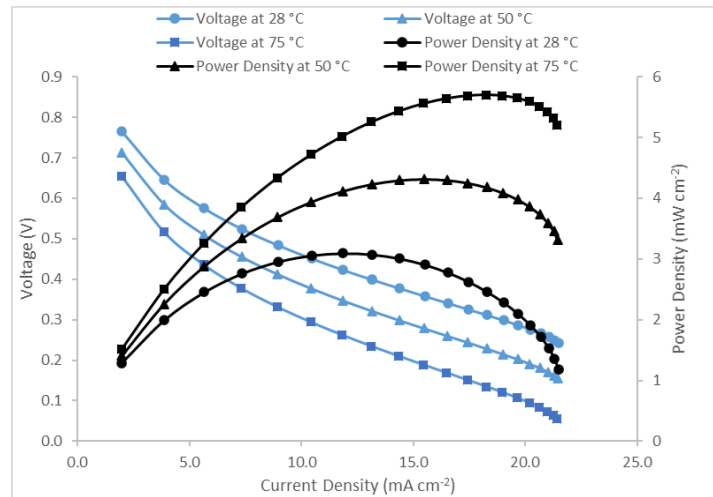


Figure 5. Influence of operating temperature on fuel cell performance based on mathematical modelling

Ethanol travelled from the ethanol tank to the membrane. The reduction of concentration depended on the travel distance at each part of the MEA. MEA consisted of the current collector, gas diffusion layer, catalyst layer and membrane. Figure 6 shows the ethanol concentration profiles of 0.5M, 1M, 1.5M, 2M, 2.5M and 3M at the anode gas diffusion layer (AGDL). From the graph, the change in ethanol concentration is minimal and appears to be constant. It was due to no chemical reaction occurring at this layer. Ethanol from the ethanol tank diffused through the anode gas diffusion layer pores went through with natural convection process [18].

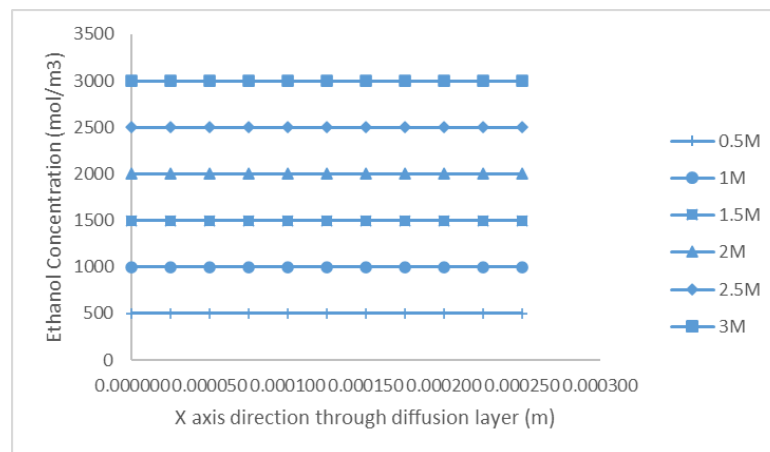


Figure 6. Ethanol concentration profiles at the gas diffusion layer for 0.5M, 1M, 1.5M, 2M, 2.5M and 3M concentration

When ethanol diffused from the ethanol tank to the gas diffusion layer, then it moved to the anode catalyst later. Figure 7 shows ethanol concentration profiles of 0.5M, 1 M, 1.5M, 2M, 2.5M and 3M at the anode catalyst layer. The ethanol concentration for all profiles significantly decreased along with the anode catalyst layer due to the electrochemical reaction between ethanol and oxygen. The generated protons at the anode travelled through the membrane electrolyte. In contrast, electrons travelled through the outer circuit, where protons and electrons combined with oxygen at the cathode to produce water [17].

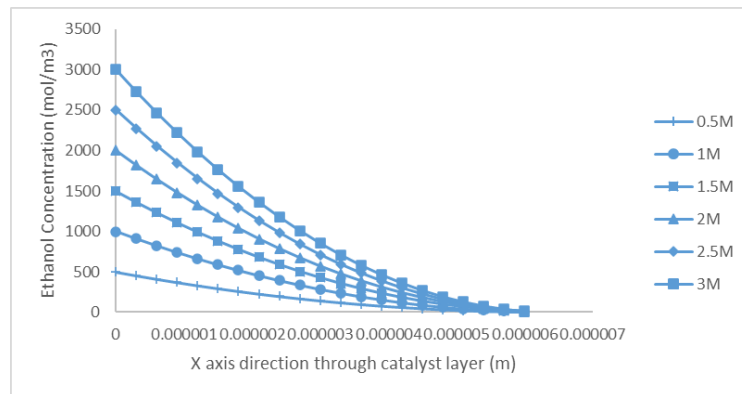


Figure 7. Ethanol concentration profiles at the anode catalyst layer for 0.5M, 1 M, 1.5M, 2M, 2.5M and 3M concentration

Figure 8 shows profiles of ethanol concentration being consumed and current density generated through the anode catalyst layer at 2M of ethanol concentration. From the graph, ethanol concentration is decreasing while current density is increasing. The current density was generated when ethanol reacted with catalyst Pd to produce a high current [16].

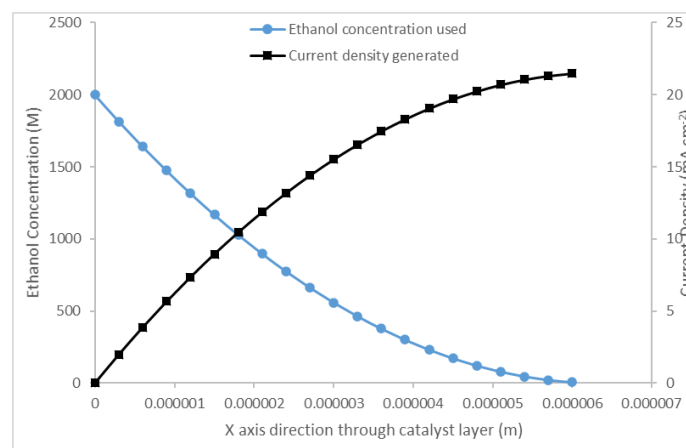


Figure 8. Ethanol concentration and current density profiles through anode catalyst layer at 2M ethanol concentration

When ethanol travelled and reacted at the anode catalyst layer, most of them had been used up. A small amount of unreacted ethanol travelled to the cathode side through the membrane. This phenomenon is called ethanol crossover. Figure 9 shows ethanol concentration profiles of 0.5M, 1M, 1.5M, 2M, 2.5M and 3 M at the membrane. This figure shows ethanol crossover where ethanol concentration is slightly reduced when travelling through the membrane and eventually moved to the cathode side. The amount of ethanol travelled through the membrane was the amount of ethanol crossover [18].

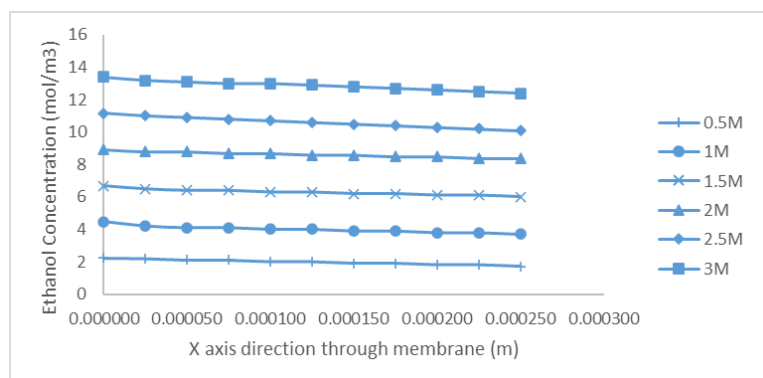


Figure 9 Ethanol concentration profiles at the membrane for 0.5M, 1M, 1.5M, 2M, 2.5M and 3 M concentration

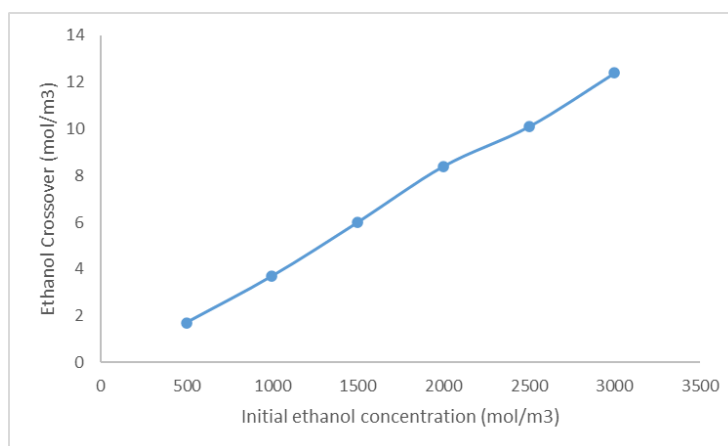


Figure 10 Ethanol cross-over profiles for 0.5M, 1M, 1.5M, 2M, 2.5M and 3M concentration

The remaining ethanol that travelled through the membrane crossed over to the cathode side. This phenomenon is called ethanol crossover. Figure 4.11 shows the amount of ethanol cross-over for 0.5M, 1 M, 1.5M, 2M, 2.5M and 3M concentrations. The higher the concentration of the ethanol, the higher the ethanol crossover. Ethanol crossover might cause problems such as mixed potential at the cathode when ethanol was oxidised to form the parasitic current. Water flooding might also occur as ethanol was directly oxidised to generate water at the cathode side [19]. Higher ethanol concentration caused higher parasitic current at the cathode side, which led to the poorer overall performance of fuel cells [20].

4. Conclusions

The mathematical model was developed for DEFC. Operating conditions such as ethanol concentrations and operating temperatures were used to simulate the mathematical model, and the results were analysed. Ethanol concentration played a vital role to achieve high-performance DEFC. Increasing the ethanol concentration led to a higher current generation in DEFC. Nonetheless, higher ethanol crossover occurred when a higher ethanol concentration was used. Thus, the modelling was unable to accurately predict the power density when ethanol concentration surpassed 2.5 M. More researches on ethanol concentration of 2.5 M and above need to be done. The highest current density produced from the fuel cell was at 21.48 mA cm⁻², with 2M of ethanol concentration. Operating temperature also affected cell performance; increasing the operating temperature increased the power density produced—the peak power density of 5.7 mWcm⁻² at 75 °C with 2M of ethanol. The ethanol mass transferred from the membrane travelled to the cathode side, which was considered ethanol crossover. The highest ethanol crossover was at 12.4 mol m⁻³ for a 3M concentration of ethanol. It proved that higher ethanol concentration led to higher ethanol crossover. The voltage and power density values were parallel for experimental and modelling, which meant mathematical modelling was successfully derived and validated the research data.

Acknowledgements

The author would like to thank Polytechnic of Kuching Sarawak for their support.

References

- [1] Mench, M. M. (2006). Fuel Cells. *Mechanical Engineers' Handbook: Energy and Power: Third Edition*, 4, 922–957. <https://doi.org/10.1002/0471777471.ch28>
- [2] Shen, S. Y. (2012). *Preparation and Characterization of Nanocatalysts for Ethanol Oxidation in Anion-Exchange Membrane Direct Ethanol Fuel Cells*. August. <http://hdl.handle.net/1783.1/7807>
- [3] Lamy, C., Rousseau, S., Belgsir, E. M., Coutanceau, C., & Léger, J. M. (2004). Recent progress in the direct ethanol fuel cell: Development of new platinum-tin electrocatalysts. *Electrochimica Acta*, 49(22-23 SPEC. ISS.), 3901–3908. <https://doi.org/10.1016/j.electacta.2004.01.078>
- [4] Lamy, Claude, Lima, A., LeRhun, V., Delime, F., Coutanceau, C., & Léger, J. M. (2002). Recent advances in the development of direct alcohol fuel cells (DAFC). *Journal of Power Sources*, 105(2), 283–296. [https://doi.org/10.1016/S0378-7753\(01\)00954-5](https://doi.org/10.1016/S0378-7753(01)00954-5)
- [5] Ekdharmasuit, P. (2020). Performance and Ethanol Crossover of Passive Direct Ethanol Fuel Cell Stack. *E3S Web of Conferences*, 141, 1–6. <http://doi.org/10.1051/e3sconf/202014101008>
- [6] Kamarudin, M. Z. F., Kamarudin, S. K., Masdar, M. S., & Daud, W. R. W. (2013). Review: Direct ethanol fuel cells. *International Journal of Hydrogen Energy*, 38(22), 9438–9453. <https://doi.org/10.1016/j.ijhydene.2012.07.059>
- [7] Song, Shuqin, Zhou, W., Liang, Z., Cai, R., Sun, G., Xin, Q., Stergiopoulos, V., & Tsiakaras, P. (2005). The effect of methanol and ethanol cross-over on the performance of PtRu/C-based anode DAFCs. *Applied Catalysis B: Environmental*, 55(1), 65–72. <https://doi.org/10.1016/j.apcatb.2004.05.017>
- [8] Andreadis, G., Stergiopoulos, V., Song, S., & Tsiakaras, P. (2010). Direct ethanol fuel cells: The effect of the cell discharge current on the products distribution. *Applied Catalysis B: Environmental*, 100(1–2), 157–164. <https://doi.org/10.1016/j.apcatb.2010.07.025>
- [9] An, L., Chai, Z. H., Zeng, L., Tan, P., & Zhao, T. S. (2013). Mathematical modeling of alkaline direct ethanol fuel cells. *International Journal of Hydrogen Energy*, 38(32), 14067–14075. <https://doi.org/10.1016/j.ijhydene.2013.08.080>

- [10] Souza, M. M. De. (2016). *Two-Dimensional Simulations Via Finite Elements Of Direct Ethanol Fuel Cells (DEFC)*. <https://doi.org/10.26512/ripe.v2i11.21271>
- [11] Gomes, R. S., & De Bortoli, A. L. (2016). A three-dimensional mathematical model for the anode of a direct ethanol fuel cell. *Applied Energy*, 183, 1292–1301. <https://doi.org/10.1016/j.apenergy.2016.09.083>
- [12] Azam, A. M. I. N., Lee, S. H., Masdar, M. S., Zainoodin, A. M., & Kamarudin, S. K. (2019). Parametric study on direct ethanol fuel cell (DEFC) performance and fuel crossover. *International Journal of Hydrogen Energy*, 8566–8574. <https://doi.org/10.1016/j.ijhydene.2018.08.121>
- [13] James, D. D., & Pickup, P. G. (2010). Effects of crossover on product yields measured for direct ethanol fuel cells. *Electrochimica Acta*, 55(11), 3824–3829. <https://doi.org/10.1016/j.electacta.2010.02.007>
- [14] Pethaiah, S. S., Arunkumar, J., Ramos, M., Al-Jumaily, A., & Manivannan, N. (2016). The impact of anode design on fuel crossover of direct ethanol fuel cell. *Bulletin of Materials Science*, 39(1), 273–278. <https://doi.org/10.1007/s12034-015-1130-6>
- [15] Ismail, A., Kamarudin, S. K., Daud, W. R. W., Masdar, S., & Hasran, U. A. (2018). Development of 2D multiphase non-isothermal mass transfer model for DMFC system. *Energy*, 152, 263–276. <https://doi.org/10.1016/j.energy.2018.03.097>
- [16] Goel, J., & Basu, S. (2015). ScienceDirect Mathematical modeling and experimental validation of direct ethanol fuel cell. *International Journal of Hydrogen Energy*, 1–11. <https://doi.org/10.1016/j.ijhydene.2015.03.082>
- [17] Gomes, R. S., Souza, M. M. De, & Bortoli, A. L. De. (2018). Accepted us t. *Chemical Engineering Research and Design*. <https://doi.org/10.1016/j.cherd.2018.05.037>
- [18] Rejal, S. Z., Masdar, M. S., & Kamarudin, S. K. (2014). A parametric study of the direct formic acid fuel cell (DFAFC) performance and fuel crossover. *International Journal of Hydrogen Energy*, 39(19), 10267–10274. <https://doi.org/10.1016/j.ijhydene.2014.04.149>
- [19] Zakaria, Z., Kamarudin, S. K., & Timmiati, S. N. (2016). Membranes for direct ethanol fuel cells: An overview. *Applied Energy*, 163, 334–342. <https://doi.org/10.1016/j.apenergy.2015.10.124>
- [20] Abdullah, S., Kamarudin, S. K., Hasran, U. A., Masdar, M. S., Aziz, A. S. A., & Hashim, N. (2021) Parametric investigation and optimization of passive direct ethanol alkaline fuel cells. *Materials Today: Proceedings*, 42(1), 259-264. <https://doi.org/10.1016/j.matpr.2021.01.279>